MOLECULAR & CELLULAR TOXICOLOGY, Vol. 2, No. 2, 126-133, June 2006

Toxicogenomics Analysis on Thioacetamide-induced Hepatotoxicity in Mice

Jung-Sun Lim[1], Sun-Young Jeong[1], Ji-Yoon Hwang[1], Han-Jin Park[1], Jae-Woo Cho[1] & Seokjoo Yoon[1]

[1]Toxicogenomics Team, Korea Institute of Toxicology, Korea Research Institute of Chemical Technology, Daejeon, Korea
Correspondence and requests for materials should be addressed to S.J. Yoon (sjyoon@kitox.re.kr)

Accepted 18 May 2006

Abstract

Thioacetamide (TA) is well known hepatotoxic and hepatocarcinogenic agent. TA also diminishes the contents of hepatic cytochrome P450 and inhibits the enzyme activity of the hepatic mixed function oxidases. TA metabolite, thioacetamide-s-oxide, is further transformed into a still unknown highly reactive metabolite that binds to macromolecules. In this study, we focused on TA-induced gene expression at hepatotoxic dose. Mice were exposed to two levels (5 mg/kg or 50 mg/kg i.p.) of TA, sampled at 6 or 24 h, and hepatic gene expression levels were determined to evaluate dose and time dependent changes. We evaluated hepatotoxicity by serum AST and ALT level and histopathological observation. Mean serum activities of the liver leakage enzymes, AST and ALT, were slightly increased compare to control. H & E and PAS evaluation of stained liver sections revealed TA-associated histopathological finding in mice. Centrilobular eosinophilic degeneration was observed at high dose-treated mice group. Hepatic gene expression was analyzed by QT clustering. Clustering of high dose-treated samples with TA suggests that gene expressional changes could be associated from toxicity as measured by traditional biomarkers in this acute study.

Keywords: Toxicogenomics, Thioacetamide, Hepatic gene expression

Thioacetamide (TA) is a well defined hepatotoxic and hepatocarcinogenic agent, which is widely used as an inducer of liver necrosis, carcinoma in laboratory animal model experiments[1]. TA also decreases the contents of hepatic cytochrome P450 (P450) and inhibits the enzyme activity of the hepatic mixed function oxidases[2]. P450 2B and 2E1 and flavin containing monooxygenase (FMO) metabolize thioacetamide to its metabolite[3,4]. In addition, it was suggested that the intermediate metabolites of TA might bind to cellular proteins by the formation of acetylimidolysine derivates[5]. The hepatotoxicity induced by thioacetamide is relatively well characterized with an emphasis in the metabolic activation[6,7]. TA also binds to several subunits of glutathione-s-transferase (GST) and inhibits the expression of class α GST[8]. The mechanism of TA was not fully understood it is considered that TA is converted in the liver to several metabolites (sulfate, acetamide, thioacetamide-*s*-oxide) in a P450 dependent metabolism[9-11]. The metabolites are further transformed into a still unknown highly reactive metabolites that bind to DNA, RNA and proteins[12], possibly changing the expression. Classical toxicology depends on descriptive histopathology and blood biochemistry to evaluate hepatic injury of a compound. These classical endpoints provide inadequate insights into the mechanism behind the observed hepatotoxicities and generally offer limited predictive value in long-term risk assessment for clinical trials[13-17]. In this paper, we investigated the effect of the well-defined hepatotoxicant TA in the gene expression and histopathological change in mouse liver.

Blood Biochemical & Histopathological Analysis

The activities of alanine aminotransferase (ALT) and aspartate aminotransferase (AST) in the serum are good indicators of the hepatotoxicity induced by TA. Levels of circulating enzymes were observed in mice receiving hepatotoxic doses of TA. However, serum level of ALT and AST were not significantly changed (Fig. 1) following TA treatment (Low 5 mg/kg or High 50 mg/kg, sampled at 6 or 24 h after treatment, respectively). Doses and duration exposure were selected from preliminary study. Hematoxylin and eosin (H & E) and PAS evaluation of stained liver sections revealed TA-induced histopathological changes in mice. Moderate centrilobular eosinophilic degeneration was present in all high dose (50 mg/kg) TA treated groups (Figs. 2, 3). Animals sacrificed 6 h post-TA dosing (high dose) had relatively severe centrilobular eosinophilic degeneration (Fig. 2C).

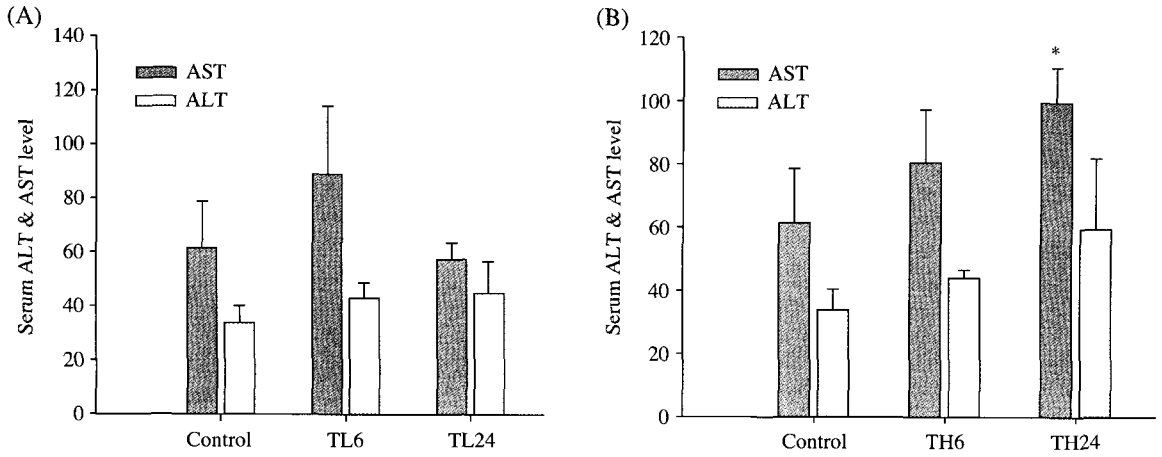

Fig. 1. Blood biochemistry observations in serum of TA treated mice. Levels of aspartate aminotransferase (AST) and alanine aminotransferase (ALT) in TA treated rats relative to those of control animals are presented for the 5 mg/kg (A) and 50 mg/kg (B) doses across the 6 and 24 h time points. Values given are means ± SD (n=3), $*P < 0.05$, *t*-test (Dunnett)

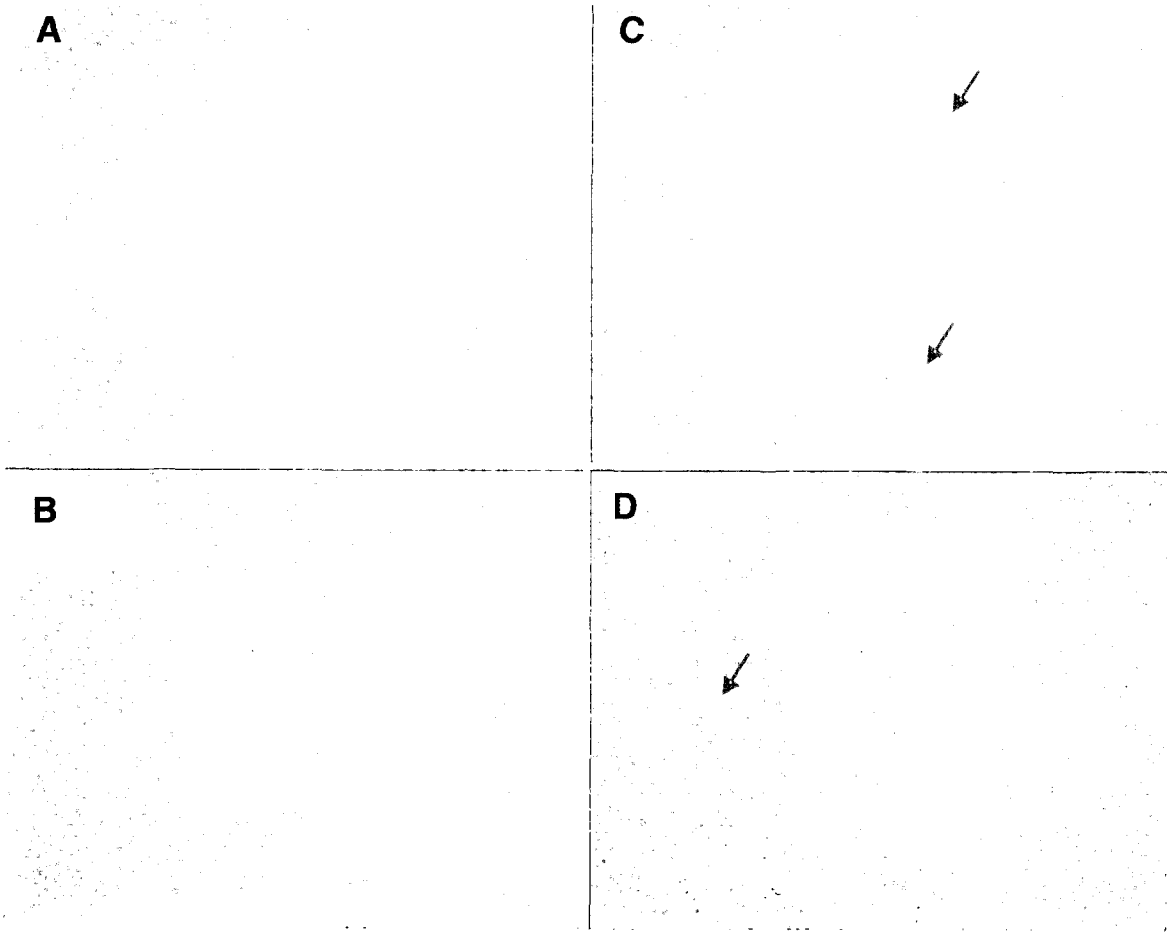

Fig. 2. Histopathology after thioacetamide treatment. Representative hematoxylin and eosin (H & E) stained histological liver sections derived from C57BL/6J mice treated with 5 mg/kg (A) or 50 mg/kg (B) after the 6 h post treatment as well as 5 mg/kg (C) or 50 mg/kg (D) after the 24 h post treatment. *Note.* Original magnification (100 ×)

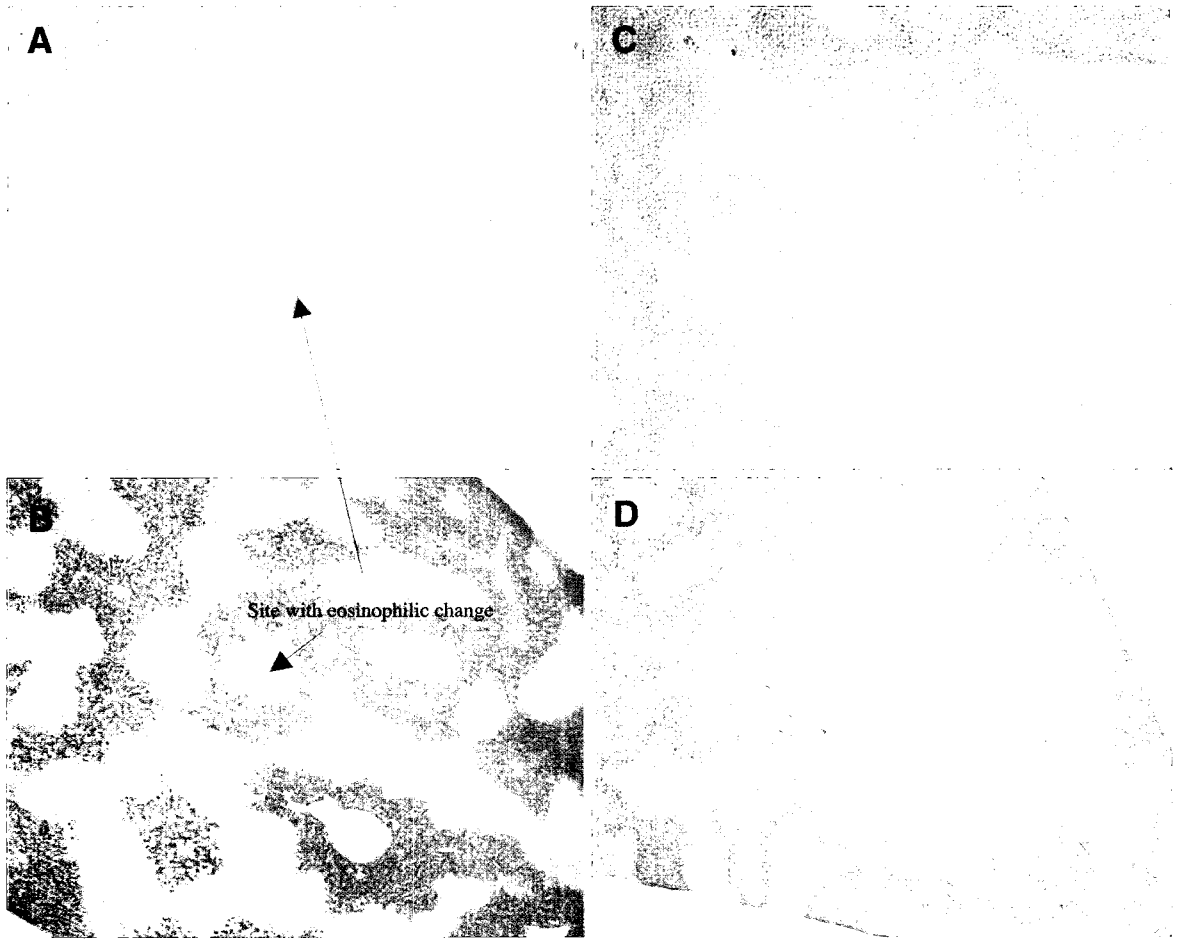

Fig. 3. Histopathology after thioacetamide treatment. Liver sections derived from C57BL/6J mice treated with 50 mg/kg after the 6 h (A and B) or 24 h (C and D) post treatment.
Note. Original magnification (40 ×), PAS stain (A and C), H & E stain (B, D)

Treatment with TA for 24 h resulted in mild centrilobular eosinophilic degeneration (Fig. 2D).

Gene Expression Analysis

RNA was isolated from the livers of TA treated mice. The RNA integrity of the RNA was determined using an Agilent 2100 bioanalyzer. DNA chip analysis was done to determine differences in hepatic gene expression between TA-and vehicle treated mice at each time and dose points. For each of the approximately 7400 genes present on TwinChip Mouse 7.4 K. Gene expression profiles of interest were significantly up-or down regulated in mice treated with TA. Treatment with hepatotoxic doses of TA caused the statistically significant, at least 2 fold up-or down regulation of many probe set on the DNA chips. Hepatic gene expression was measured 6 or 24 h following low or high dose TA treatment. Gene expression patterns were showed in self-organizing map (SOM) (Fig. 4). The SOM is a clustering technique similar to *k*-means clustering. However, SOMs illustrate the relationship between groups by arranging them in a two-dimensional map in addition to dividing genes into groups based on expression patterns. SOMs are useful for visualizing the number of distinct expression patterns in genomic data and determining which of these patterns are variants of one another[18,19]. To easily access analyzed data, we also applied the QT (quality threshold >0.95) clustering which is an algorithm that groups genes into high quality clusters. Gene expression patterns within the data were initially analyzed by QT clustering for the two times and doses points (Fig. 4). Clustering set 1 (Fig. 4A) shows significantly increased gene expression pattern at high dose-6 h group. Clustering set 2 (Fig. 4B) shows increased gene expression pattern in

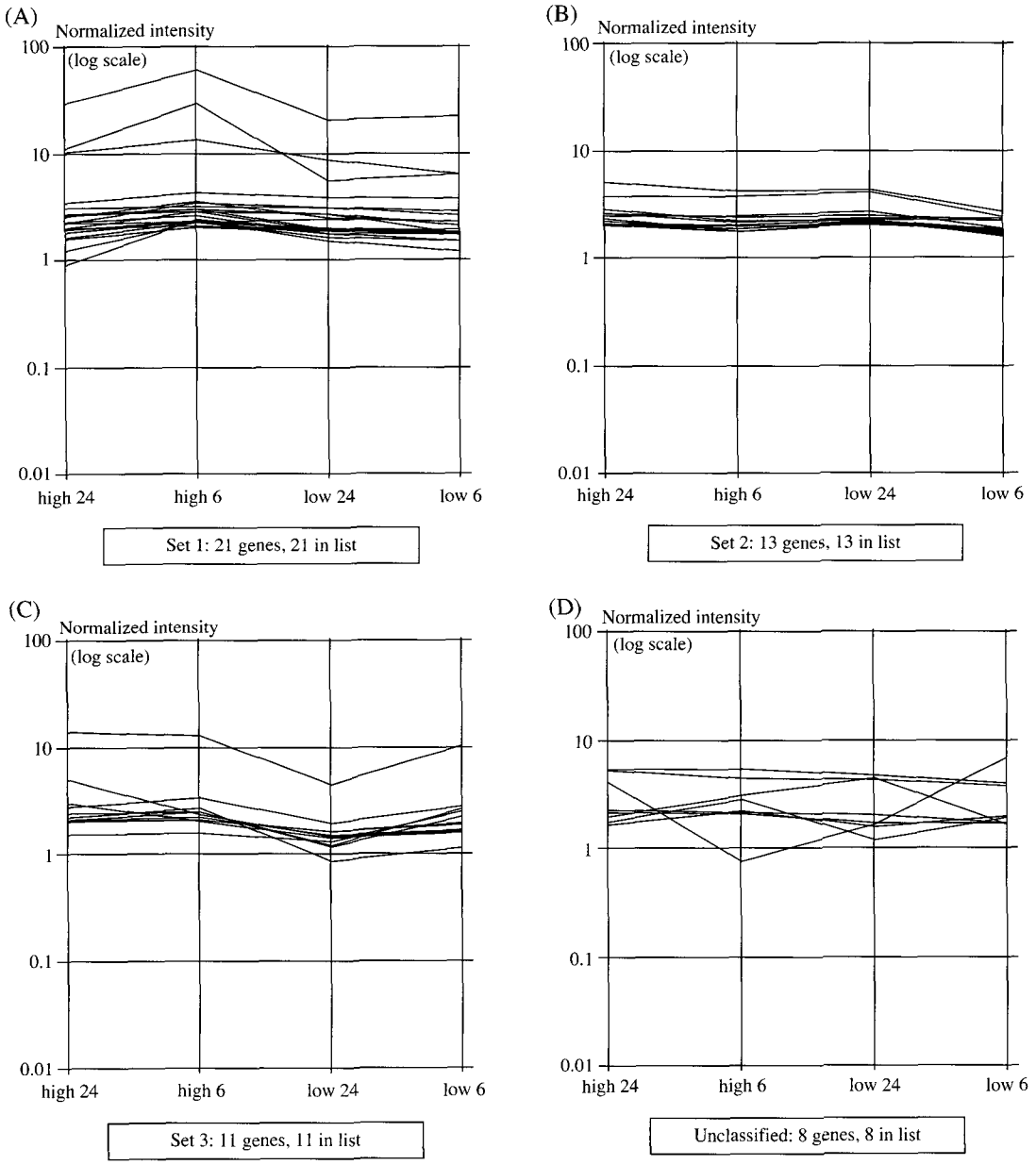

Fig. 4. Viewing self-organizing map clustering results. 2-fold up and/or down regulated genes from *t*-test ($P<0.05$), Total 53 genes were clustered with quality threshold 0.9 (correlation). X-axis represented for treatment dose and duration (hrs), Y-axis represented for fold change relative to vehicle treated group.

following order (low6 < low24 < high6 < high24). Clustering set 3 (Fig. 4C) shows relatively decrease gene expression pattern in low 24 group. Serum amyloid A (Saa) 3 (Cluster set 1, Table 1), an acute phase reactant (APR) protein, is induced in liver during systemic inflammation. Saa3, an isoform of Saa, induced in both liver and extra hepatic sites in response to proinflammatory stimuli such as cytokines[20]. Its levels are highest (60 folds) in high dose (50 mg/kg) at 6 h. Also, other groups showed higher expression level (20-30 folds) of Saa3. Granulins (grns, Cluster set 1, Table 1), also called epithelins, are cystein rich polypeptide with pleiotropic effects on epithelial cell growth. It also highly expressed after TA treatment. Thrombospondin (Thb) 2 (Cluster set 2, Table 2) is multifunctional matricellular glycoprotein with anti-angiogenic properties and are expressed in a wound repair model. Nicotinamide *N*-

Table 1. Gene lists from Fig. 4A.

Set 1					
Accession number	High 24	High 6	Low 24	Low 6	Gene description
AI646683	29.230	60.390	20.460	22.060	Saa3, serum amyloid A 3
AI838885	1.957	2.823	1.869	1.908	Nme6, expressed in non-metastatic cells 6
AI846708	2.533	3.532	2.473	2.257	Rpn1, ribophorin I
AA458241	0.900	2.411	1.829	1.685	G0s2, G0/G1 switch gene 2
AI645666	1.225	2.262	1.753	1.462	Spg20, spastic paraplegia 20
AI845868	1.629	2.241	2.390	2.230	Rmcs1, response to metastatic cancers 1
AI047920	2.688	2.820	2.691	2.083	LOC226856, hypothetical protein
AI846605	2.187	3.448	3.028	2.576	Grn, granulin
AI837104	2.247	2.581	1.736	1.725	Signal transducer and activator of transcription 1
AI450593	2.649	2.961	1.916	1.915	D6Bwg1452e, DNA segment, Chr 6
AI507030	1.907	2.311	1.857	1.791	MGC6998, hypothetical protein
AI527294	10.170	13.470	8.560	6.388	Apcs, serum amyloid P-component
AA798311	2.186	2.222	1.937	1.784	DnaJ homolog, subfamily c, member 12
AI415648	3.445	4.276	3.830	3.733	Hpxn, hemopexin
AA881525	10.940	29.500	5.561	6.335	Saa3, serum amyloid A 3
AI480753	3.067	3.150	3.030	2.786	Cyt19-pending,methyltransferase
AI842506	1.943	2.043	1.897	1.907	P4hb, prolyl 4-hydroxylase, beta polypeptide
AI327250	2.604	2.954	2.625	1.762	Fgb, fibrinogen, B beta polypeptide
AI836381	1.585	2.039	1.840	1.725	Actg, actin, gamma, cytoplasmic 1
AI119664	1.778	2.333	1.476	1.178	Cml2, camello-like 2
AI303526	1.880	2.269	1.590	1.491	Fga, fibrinogen, alpha polypeptide

Table 2. Gene lists from Fig. 4B.

Set 2					
Accession number	High 24	High 6	Low 24	Low 6	Gene description
W89831	5.108	4.122	4.217	2.667	Fga, fibrinogen, alpha polypeptide
AA153731	2.62	2.138	2.326	2.316	Tumor necrosis factor receptor subfamily, member 7
AI845834	1.998	1.759	2.046	1.704	Thbs2, thrombospondin 2
AI848758	2.094	1.968	1.994	1.848	Lcat, lecithin cholesterol acyltransferase
AI605164	2.061	2.032	2.262	1.582	Klra21, killer cell lectin-like receptor
AI121183	2.342	1.762	2.1	1.604	RIKEN cDNA 9130019P20 gene
AA062129	2.831	2.215	2.258	2.167	Itih3, inter-alpha trypsin inhibitor, hea
AI843247	2.078	1.833	2.193	1.776	–
AI526937	3.7	3.684	4.084	2.354	Nnmt, nicotinamide N-methyltransferase
AI121911	2.604	2.404	2.439	2.199	Adh8-pending, alcohol dehydrogenase 8
AI843252	2.018	1.838	2.129	1.739	Serping1, serine (or cysteine) proteinase
AI894169	2.166	1.834	2.127	1.639	Pzp, pregnancy zone protein
AA049060	2.417	2.458	2.631	1.836	Itih4, inter alpha-trypsin inhibitor

Table 3. Gene lists from Fig. 4C.

Set 3					
Accession umber	High 24	High 6	Low 24	Low 6	Gene description
AA146551	1.539	1.552	1.291	2.448	E130305N23Rik, RIKEN cDNA
AI323108	2.042	2.081	1.613	1.854	Pcx, pyruvate carboxylase
AA049185	2.057	2.169	1.478	1.659	Signal transducer and activator of transcription
AA796822	2.016	2.041	1.631	1.89	Siat4a, sialyltransferase 4A
AI837846	2.071	2.454	1.149	2.172	Fdps, farnesyl diphosphate synthetase
AI838290	2.718	3.347	1.919	2.73	Arginine-rich, mutated in early stage tumors
AI061004	4.866	2.287	1.457	1.621	Zfp291, zinc finger protein 291
BC048497	2.363	2.433	1.182	2.55	Fdps, farnesyl diphosphate synthetase
AI019469	2.974	2.014	1.385	1.572	Glul, glutamate-ammonia ligase
AI504330	13.78	12.52	4.429	10.16	Plxnb1, plexin B1
AI322955	2.169	2.634	0.858	1.111	Selenbp1, selenium binding protein 1

Table 4. Gene lists from Fig. 4D.

Unclassified					
Accession number	High 24	High 6	Low 24	Low 6	Gene description
AK076062	1.771	2.835	1.184	1.925	Farnesyl diphosphate farnesyl transferase 1
AI838222	2.125	2.045	1.715	1.694	Fkbp8, FK506 binding protein 8
AA061673	5.167	4.381	4.331	3.735	DXHXS253E, DNA segment, Chr X
AK088691	1.647	2.194	1.554	1.936	Actb, actin, beta, cytoplasmic
AI414506	1.983	3.079	4.45	1.676	Hist1h1c, histone 1, H1c
AI663940	5.403	5.294	4.681	3.944	Gabt2, gamma-aminobutyric acid
AI648728	4.003	0.760	1.643	6.686	Iinsulin-like growth factor binding protein
AI467075	2.243	2.144	2.018	1.687	Grp58, glucose regulated protein

methylstransferase (Nnmt) (Cluster set 2, Table 2) is methyltransferase structural and functionally related to thioether *S*-methlytransferase and phenylethanolamine *N*-methyltransferase. Nmnt has broad substrate specificity. It catalyzes the N-methylation of nicotinamide, pyridines, and other structural analogs and is involved in the biotransformation of many drugs and xenobiotic compounds[21]. Pyruvate carboxylase (PC) (Cluster set 3, Table 3) is a biotin-dependent enzyme and is involved in gluconeogenesis by converting pyruvate to oxalacetate[22]. Farnesyl diphosphate synthase (Fdps) (Cluster set 3, Table 3) is a key enzyme in isoprenoid biosynthesis which supplies sesquiterpene precursors for several classes of essential metabolites including sterols, dolichols, ubiquinones and carotenoids as well as substrates for farnesylation of proteins. It catalyzes the sequential head-to-tail condensation of two molecules of isopentenyl diphosphate with dimethylallyl diphosphate[23].

Discussion

The purpose of this study was to elucidate whether generation of hepatotoxicant associated gene expression with phenotype dependent dose and time points, using microarray technology, would get information of hepatotoxic mechanism of TA. TA is frequently used as an experimental model of liver damage, which causes necrosis or cirrhosis, depending on the dose and duration of administration[24, 25]. Toxicity of TA depends on bioactivation, mainly associated with CYP2E1 and FMO. Fulminant hepatic failure is a severe complication of acute hepatitis of various etiologies, characterized by massive hepatic necrosis. TA, well defined hepatotoxin, is well known to induce hepatic failure within a short period of time after the administration of the drug; it undergoes extensive metabolism to acetamide and thioacetamide-*S*-oxide by mixed function oxidase system. Acetamide does not have liver necrotizing properties while thioacetamide-*S*-oxide is further metabolized, at least in part, by P450 monooxygenase to sulfene, thioacetamide-*S*-dioxide. Thioacetamide-*S*-dioxide is a very highly reactive compound. Its binding to tissue macromolecules might induce hepatic necrosis. We examined blood biochemical test and histopathological analysis for evaluation of TA-induced hepatotoxicity. In results, hepatic enzymes, AST and ALT, showed slightly increased at TA-treated group. In histopathological data, high dose-6 hr group showed severe centrilobular eosinophilic degeneration. However, high dose-24 h group showed relatively mild eosinophilic degeneration. It suggested that certain regeneration process was occurred at the TA-treated group. Hepatic gene expression was analyzed by QT clustering. Clustering of high dose-treated samples with TA suggests that gene expressional changes could be associated from toxicity as measured by traditional biomarkers (histopathology and blood biochemistry) in this acute study.

Methods

Animals

Approximately 12-week-old C57BL/6J male mice were kept in a 10 h light/dark cycle animal room with controlled temperature and humidity for 2-week prior to experiment. Those mice maintained on a standard diet and weighed from 24 to 27 g (mean $\pm$ SD, 25.33 $\pm$ 1.07) in these experiments. Thus the terminal body weights and liver weights were recorded. Saline-(vehicle) and TA-treated groups consisted of 3 mice at each point, respectively. Those were exposed intraperitoneally to two levels (5 or 50 mg/kg) of Thioacetamide (Sigma, U.S.A.) that sampled at 6 or 24 h.

Biochemical Analysis

After the mice were anesthetized with diethylether, blood was gathered through the inferior vena cava.

For biochemical parameters, commercial kits (kits58-UV, kits 59-UV; Sigma, U.S.A.) were used in this study. The activities of alanine aminotransferase (AST), aspartate aminotransferase (ALT) were measured using the Shimadzu automatic biochemistry analyzer (Shimadzu, Japan) at each time points as indicated above.

Histopathology

The liver samples were harvested from the 12-week-old mice, fixed in 10% neutral buffered formalin, and embedded in paraffin. For histopathological analysis, the sections were cut 4 μm in thickness (RM2165 Microtome, Leica, Germany), stained with H & E or PAS and examined with a light microscope (Nikon E400, Japan).

Isolation of RNA

The left lateral lobe of the liver was processed for RNA extraction. For cDNA microarray analysis, total RNA was extracted using TRIzol reagent (InVitrogen, U.S.A.) and purified using RNeasy total RNA isolation kit (Qiagen, Germany) according to the manufacturer's instructions. Total RNA was quantified by NanoDrop (NanoDrop, U.S.A.) and its integrity was assessed by running 2100 Bioanalyzer (Agilent, U.S.A.). The remaining portion of the liver was retained frozen for future study.

cDNA Microarray

Fluorescent-labeled cDNA for microarray analysis was prepared by the reverse-transcription of total RNA in the presence of aminoallyl-dUTP followed by the coupling of Cy3 or Cy5 dyes (Amersham Pharmacia, U.S.A.). Single-stranded cDNA probes were purified using a PCR purification kit (Qiagen, Germany). Probes were resuspended in hybridization solution containing 50% formamide, 5X SSC, 0.1% SDS. The TwinChip Mouse-7.4K cDNA microarray (Digital Genomics, Korea) was hybridized with the fluorescent-labeled cDNAs at 42°C in a humid chamber.

Analysis of Fluorescence Spots

After the washing procedure the slides were scanned using ScanArray Lite (PerkinElmer Life Sciences, U.S.A.). Scanned images were analyzed with GeneSpring Software version 7.0 (Silicon Genetics, U.S.A.) to obtain gene expression ratios. Logged gene expression ratios were normalized by LOWESS regression. Only genes whose expression was above 2-fold induction or below 2-fold repression by TA treatment compared with controls were considered for statistical analysis. Significant differences between control and treatment doses were determined using *t*-test. *P* values <0.05 were considered statistically significant.

Data Analysis, Data Annotation

Lists of the significantly differentially regulated genes upon TA treatment were further analyzed using Genespring software. Hierarchical clustering was applied to identify similarly regulated groups and to determine treatment-related effects. The hierarchical clustering of Genespring program class together experiments of genes by clustering based upon expression profile similarities. Information was collected from different databases, including Unigene from the National Center for Biotechnology Information (NCBI) or NetAffx Analysis Center.

Statistical Analysis

Data are expressed as the mean $\pm$ SD of samples. Comparisons of differences were performed by using analyses of variance (ANOVA). $P<0.05$ was considered statistically significant with Dunnett multiple comparison test.

Acknowledgments

This work was supported by the Ministry of Science and Technology for the 2005 Advanced Project for an International Accreditation of the Preclinical Safety Evaluation System for Korea Institute of Toxicology.

References

1. Spira, B. & Raw, I. Differentially expressed genes in the liver of thioacetamide treated rats. *Comp. Biochem. Physiol. C Toxicol. Pharmacol.* **135**(2), 129-135 (2003).
2. Barker, E.A. & Smuckler, E.A. Altered microsome function during acute thioacetamide poisoning. *Mol. Pharmacol.* **8**, 318-326 (1972).
3. Hunter, A.L., Holscher, M.A. & Neal, R.A. Thioacetamide-induced hepatic necrosis. I. Involvement of the mixed-function oxidase enzyme system. *J. Pharmacol. Exp. Ther.* **200**, 439-448 (1977).
4. Wang, T., Shankar, K., Ronis, M.J.J. & Mehendale, H.M. Potentiation of thoiacetamide liver injury in diabetic rats is due to induced CYP2E1. *J. Pharmacol. Exp. Ther.* **294**, 473-479 (2000).
5. Dyroff, M.C. & Neal, R.A. Identification of the major protein adduct formed in rat liver after thioacetamide administration. *Cancer Res.* **41**, 3430-3435 (1981).
6. Porter, W.R. & Neal, R.A. Metabolism of thioacetamide and thioacetamide S-oxide by rat liver micro-

somes. *Drug Metab. Dispos.* **6**, 379-388 (1978).
7. Dyroff, M.C. & Neal, R.A. Studies of the mechanism of metabolism of thioacetimide s-oxide by rat liver microsomes. *Mol. Pharmacol.* **23**, 219-227 (1983).
8. Spira, B. & Raw, I. The effect of thioacetamide on the activity and expression of cytosolic rat liver glutathione-S-transferase. *Mol. Cell Biochem.* **211**(1-2), 103-110 (2000).
9. Nygaard, O., Eldjarn, L. & Nakken, K.F. Studies on the metabolism of thioacetamide-*s*-35 in the intact rat. *Cancer Res.* **14**, 625-628 (1954).
10. Rees, K.R., Rowland, G.F. & Varcoe, J.S. Metabolism of tritiated thioacetamide in rat. *Int. J. Cancer* **1**, 197 (1966).
11. Porter, W.R., Gudzinowicz, M.J. & Neal, R.A. Thioacetamide-induced hepatic necrosis. II. Pharmacokinetics of thioacetamide and thioacetamide-*s*-oxide in the rat. *J. Pharmacol. Exp. Ther.* **208**, 386-391 (1979).
12. Vadi, H.V. & Neal, R.A. Microsomal activation of thioacetamide-*s*-oxide to a metabolite (s) that covalently binds to calf thymus DNA and other polynucleotides. *Chem. Biol. Interact.* **35**, 25-38 (1981).
13. Waring, J.F. *et al.* Clustering of hepatotoxins based on mechanism of toxicity using gene expression profiles. *Toxicol. Appl. Pharmacol.* **175**, 28-42 (2001).
14. Ruepp, S.U. *et al.* Genomics and proteomics analysis of acetaminophen toxicity in mouse liver. *Toxicol. Sci.* **65**, 135-150 (2002).
15. Hamadeh, H.K. *et al.* Gene expression analysis reveals chemical-specific profiles. *Toxicol. Sci.* **67**, 219 -231 (2002).
16. Hamadeh, H.K. *et al.* Prediction of compound signature using high density gene expression profiling. *Toxicol. Sci.* **67**, 232-240 (2002).
17. Huang, Q. *et al.* Gene expression profiling reveals multiple toxicity endpoints induced by hepatotoxicants. *Mutat. Res.* **549**, 147-168 (2004).
18. Kohonen, T. The self-organizing map. *Proc. IEEE.* **78** (9), 1464-1480 (1990).
19. Tamayo, P. *et al.* Interpreting patterns of gene expression with self-organizing maps; Methods and application to hematopoietic differentiation. *Proc. Nat. Acad. Sci. USA.* **96**, 2907-2912 (1999).
20. Wilson, *et al.* Pulmonary and systemic induction of SAA3 after ventilation and endotoxin in preterm lambs. *Pediatr. Res.* **58**, 1204-1209 (2005).
21. Alston, T.A. & Abeles, R.H. Substrate specificity of nicotinamide methyltransferase isolated from porcine liver. *Arch. Biochem. Biophys.* **260**, 601-608 (1988).
22. Attwood, P.V. The structure and the mechanism of action of pyruvate carboxylase. *Int. J. Biochem. Cell. Biol.* **27**, 231-249 (1995).
23. Attucci, S., Aitken, S.M., Gulick, P.J. & Ibrahim, R.K. Farnesyl pyrophosphate synthase from white lupin: molecular cloning, expression, and purification of the expressed protein. *Arch. Biochem. Biophys.* **321**, 493-500 (1995).
24. Bruck, R. *et al.* The hydroxyl radical scavengers dimethylsulfoxide and dimethylthiourea protect rats against thioacetamide-induced fulminant hepatic failure. *J. Hepatol.* **31**, 27-38 (1999).
25. Bruck, R. *et al.* Melatonin inhibits nuclear factors kappa B activation and oxidative stress and protects against thioacetamide induced liver damage in rats. *J. Hepatol.* **40**, 86-93 (2004).